Preparation, Characterization, and Protein Loading Properties of *N*-Acyl Chitosan Nanoparticles

Youngjin Cho,[1] Jun Tae Kim,[2] Hyun Jin Park[1]

[1]*College of Life Sciences and Biotechnology, Korea University, Anam-Dong, Seongbuk-gu, Seoul 136-701, Republic of Korea*
[2]*Department of Food Science and Technology, Keimyung University, Daegu 704-701, Republic of Korea*

Received 30 November 2010; accepted 12 May 2011
DOI 10.1002/app.34931
Published online 18 October 2011 in Wiley Online Library (wileyonlinelibrary.com).

ABSTRACT: Various *N*-acyl chitosans with propionyl-, hexanoyl-, nonanoyl-, lauroyl-, pentadecanoyl-, and stearoyl-groups were synthesized and self-aggregated *N*-acyl chitosan nanoparticles (CSNPs) were prepared by sonication. By the modification with *N*-acyl groups, CSNPs increased their hydrophobic character and changed its structural features to be more suitable as a delivery carrier. The mean diameters of bovine serum albumin (BSA)-loaded *N*-acyl CSNPs ranged from 138 to 551 nm. Uniform particle size distribution of BSA-loaded *N*-acyl CSNPs was observed. The protein loading efficiency of *N*-acyl CSNPs was about 94–95% with lower BSA concentration (0.1 mg/mL) and not significantly different with acyl chain length. With higher BSA concentration (1.0 mg/mL), however, the highest protein loading efficiency was observed with lauroyl and pentadecanoyl CSNPs. The results suggest that lauroyl and pentadecanoyl CSs are interesting candidates for protein delivery system. © 2011 Wiley Periodicals, Inc. J Appl Polym Sci 124: 1366–1371, 2012

Key words: *N*-acyl chitosan; BSA; nanoparticle; protein loading efficiency

INTRODUCTION

Protein drugs or pharmaceuticals have become a key component of modern medical care with development of recombinant technology. However, their oral administration and use in further applications has been hampered by the chemical and physical instability of proteins.[1] Most protein-based drugs are still used in pill form or are injected due to their instability. Studies have sought to design effective delivery systems to protect protein drugs and improve methods of drug administration.[2–6] Polymeric nanoparticles (NPs) have become a reliable vehicle of delivery in site-specific drug targeting, controlled release, and stabilization of labile molecules such as proteins, peptides and DNA.[7–10] Poly(ethylene glycol) (PEG)-modified gelatin NPs[9] and thermally responsive hydrogel NPs using poly(acrylic acid) (PAAc) and poly(*N*-isopropylacrylamide) (PNIPAM)[10] have been developed. Chitosan (CS) has attracted interest as a protein carrier because of its biodegradable, biocompatible, nontoxic, and mucoadhesive features, as well as its efficient permeation across absorptive epithelia.[11–17]

CS is a linear polysaccharide consisting of β1,4-linked 2-amino-2-deoxy-D-glucose (D-glucosamine) and 2-acetamido-2-deoxy-D-glucose (*N*-acetyl-D-glucosamine) units. It is the second most abundant biopolymer in nature after cellulose. Uniquely, CS is positively charged in an aqueous environment,[18] which enables its interaction with negatively charged sialic acid groups of mucin, prolonging the contact time between the core material and cell wall surface.[19,20] CS-based delivery systems have been studied for the mucosal delivery of polar drugs, peptides, proteins, vaccines, and DNA using various methods including crosslinking, desolvation, self-assembly, and ionic interaction.[21–23]

There are two major limitations in CSNPs as a delivery system. The first limitation is the hydrophilicity and high solubility in an acidic environment, which promotes the ready degradation of the CSNPs in the harsh acidic environment of the stomach, proteolytic breakdown in the gastrointestinal tract, and poor permeability across the gastrointestinal mucosa. These obstacles must be overcome if CSNPs are to be used for the effective delivery of their payload into the blood stream and for oral administration.[24] For this reason, hydrophobic biopolymers such as poly(lactide-*co*-glycolide) (PLGA) and poly(lactic acid) (PLA) are popularly used as a wall material of the delivery system. PLGA nanospheres can improve the stability of the enclosed proteins[25] and the transport of protein through the nasal mucosa is significantly affected by the surface properties of the PLA-

Correspondence to: H. J. Park (hjpark@korea.ac.kr).
Contract grant sponsor: Korea Health 21 R and D Project, Ministry of Health and Welfare, Republic of Korea; contract grant number: A050376.

poly(ethylene glycol) (PEG) nanoparticles.[26,27] CS's hydrophilic nature and high solubility in an acidic condition can be easily modified to various and more hydrophobic derivatives because of the presence of reactive amino and hydroxyl groups. Various hydrophilic or hydrophobic chitosan derivatives such as poly(ethylene oxide)-CS, linoleic acid-modified CS, polyelectrolyte carboxymethyl konjac glucomannan-CS, and PLGA-lecithin CS have been developed and applied as delivery systems.[14–16,28,29]

The second limitation is the lowered protein loading efficiency with higher protein concentration. For example, one study reported that the loading efficiency of linoleic acid-modified CSNPs was only 20% with a bovine serum albumin (BSA) concentration of 1 mg/mL, while the loading efficiency was 99% with lower BSA concentrations.[16] Among the CS derivatives with potential use in a delivery system, *N*-acyl CS represents an interesting candidate due to its amphiphilic nature and blood compatibility.[30]

In this study, CS was firstly modified to *N*-acyl CS using acyl chlorides or anhydrides to introduce hydrophobicity for use as matrix for a self-aggregation and protein loading. *N*-acyl CSNPs were prepared by a self-aggregation method and BSA was loaded into *N*-acyl CSNPs using a sonication. *N*-acyl modified CSNPs were characterized using Fourier transform infrared spectroscopy (FTIR), ^{1}H-nuclear magnetic resonance (NMR) spectroscopy, fluorescence, light scattering, and scanning electron microscopy (SEM). The protein loading efficiency of *N*-acyl CSNPs was also investigated as a function of BSA concentration.

EXPERIMENTAL

Materials

CS was purchased from Sigma-Aldrich Chemie (Steinheim, Germany). The molecular weight (MW) of CS determined by gel permeation chromatography was 5.23×10^5 and its degree of deacetylation (DOD) determined by FTIR and ^{1}H-NMR[31,32] was 84.9%. Propionic anhydride, hexanoic anhydride, nonanoyl chloride, lauroyl chloride, pentadecanoyl chloride, and stearoyl chloride were purchased from Sigma-Aldrich Chemie and Tokyo Kasei Kogyo (Tokyo, Japan). BSA was purchased from Irvine Scientific (Irvine, CA, USA). All other chemicals were of analytical grade and were used as received.

Synthesis of *N*-acyl CS

CS solution was prepared by dissolving 1.5 g CS in 150 mL of a mixture of 0.6% aqueous acetic acid and methanol. A molar equivalent of propionic anhydride, hexanoic anhydride, nonanoyl chloride, lauroyl chloride, pentadecanoyl chloride, or stearoyl chloride was added drop-wise to the CS solution with magnetic stirring at room temperature for 5 h. The mixture was poured into the same volume of the mixing solution of methanol and ammonia in a 7 : 3 ratio. The precipitated CSs were filtered and rinsed with distilled water, methanol, and ether. Then, they were dried at 50°C under vacuum overnight. The CS derivatives obtained by the reactions with propionic anhydride, hexanoic anhydride, nonanoyl chloride, lauroyl chloride, pentadecanoyl chloride, and stearoyl chloride were coded as 3-, 6-, 9-, 12-, 15-, and 18-CS, respectively.

FTIR spectroscopy

The FTIR spectra of the *N*-acyl-modified CSs were obtained using a model 430 FTIR spectrometer (Jasco, Tokyo, Japan) as previously described.[33] The CS samples had been previously ground and mixed with potassium bromide (KBr), and prepared as pellets by compression under a force of 5 tons in a hydraulic press. Each spectrum was obtained by the averaging of 30 scans at a resolution of 2 cm^{-1} in the wavelength range of 3800–400 cm^{-1}.

^{1}H-NMR spectroscopy

^{1}H-NMR spectra of unmodified CS and *N*-acyl-modified CS samples were recorded on an ARX 300 spectrometer (Bruker, Billerica, MA) at 25°C. CS samples were dissolved in 1% (v/v) CD_3COOD in deuterium oxide to prepare the final concentration of 30 mg/mL. The measurement conditions were 500 Hz spectral window, 32,000 data points, 30° pulse angle, 2.03 s acquisition time, and 32 scans with a delay of 1 s between each scan.

Preparation of *N*-acyl CSNPs

N-acyl CSNPs were prepared by suspending 30 mg of *N*-acyl CS in 30 mL of phosphate buffered saline (PBS, pH 7.4). The suspension was incubated at 38°C for 24 h prior to the addition of BSA to concentrations ranging from 0.1 to 1.0 mg/mL using a model UH-600 ultrasonic probe homogenizer (SMT, Tokyo, Japan) at 20 W for 2 min. *N*-acyl CSNP formed by self-aggregation.[15]

Fluorescence measurement

Pyrene was used as a hydrophobic probe. Pyrene was purified by repeated recrystallization from ethanol and vacuum-dried at 20°C. A pyrene solution was prepared by dissolving the purified pyrene in ethanol at a concentration of 0.4 mg/mL. About 20 μL of the solution was added to a 20 mL test tube and the

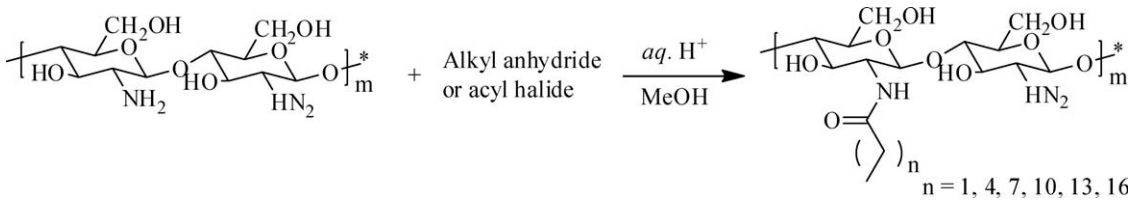

Figure 1 Synthetic scheme of *N*-acyl CSs.

ethanol was driven off under a stream of nitrogen gas. Two milliliters of *N*-acyl CSNP dispersion was added to the test tube, bringing the final concentration of pyrene to 2 μ*M*. The mixture was incubated for 3 h in a 65°C water bath prior to transfer to a BS-10 shaking water bath (Jeio Tech, Seoul, Korea) overnight at 20°C. Pyrene emission spectra were obtained using a model RF-5301PC fluorescence spectrophotometer (Shimadzu, Kyoto, Japan). The probe was excited at 343 nm and the emission spectrum was collected in the range of 360–500 nm at an integration time of 1.0 s. The excitation and emission slit opening were 15 and 1.5 nm, respectively.[15]

Particle size distribution

Particle size distribution of a 0.3% (w/v) *N*-acyl CSNP dispersion in PBS was determined using quasielestic laser light scattering with a Malvern Zetasizer (Malvern Instruments Limited, Malvern, UK). Three milliliters of the *N*-acyl CSNP dispersion was added to polystyrene latex cells, and the particle size and size distribution were measured at 25°C with a detector angle of 90°, wavelength of 633 nm, refractive index of 1.33, and real refractive index of 1.59. Each sample was measured in triplicate.

Surface morphology by SEM

The surface morphology of BSA-loaded *N*-acyl CSNPs was examined using a SEM (Hitachi, Tokyo, Japan). *N*-acyl CSNP samples were loaded on the SEM mount with double-sided adhesive carbon tape and the specimens were coated with a thin layer of platinum (~ 3–5 nm) for 100 s and at 30 W. SEM was conducted at a scanning voltage of 15 kV voltage. The resulting micrographs were magnified 3,000–18,000 times.

Protein loading efficiency of *N*-acyl CSNPs

BSA solution was added to 2 mL of CSNP solution in such a way that BSA concentration ranged from 0.1 to 1.0 mg/mL. The prepared solutions were incubated at 25°C for 24 h and were centrifuged at 20,000 × *g*, 4°C, 30 min to separate the unloaded BSA (supernatant) and BSA-loaded NPs. The quantity of unloaded BSA present in the supernatant was determined by ultraviolet spectroscopy at 280 nm. As a control, the supernatant of unloaded NPs was used. Protein loading efficiency of *N*-acyl CSNPs was determined using eq. (1):

$$\text{Loading efficiency (LE)} = \frac{(A - B)}{A} \times 100, \qquad (1)$$

where A is the initial BSA amount in the solution and B is the free BSA amount in the supernatant.

RESULTS AND DISCUSSION

Synthesis and characterization of *N*-acyl CS

Figure 1 presents the schematics of the synthesis of *N*-acyl CS with various elongations (3-, 6-, 9-, 12-, 15-, and 18-CS). Free amine groups in CS can react with the carboxyl groups of alkyl anhydrides or acyl halides to form an amide bond. Figure 2 shows the FTIR spectra of *N*-acyl-modified CSs (3-CS, 6-CS, and 18-CS). The characteristic absorption peaks of *N*-acyl-modified CS were observed at 3000–3800cm^{-1} for -OH and -NH_2, at 2918cm^{-1} and 2848cm^{-1} for C-H stretching and at 1068 cm^{-1} for C-O stretching vibration. The absorption of C-H stretching of *N*-acyl CS at 2918 cm^{-1} and 2848 cm^{-1} increased with elongations of the alkyl side chain. Two major peaks at 1662 cm^{-1} and 1556 cm^{-1} were assigned to C=O stretching (amide I) and *N*-H bending vibration (amide II), respectively. Figure 3 shows the ^{1}H-NMR spectra of the control CS and *N*-acyl CS (12-CS). The control CS displayed two major peaks at 1.8 ppm and 2.9 ppm [Fig. 3(a)], which are assigned to three *N*-acetyl protons of *N*-acetylglucosamine (GlcNAc) and the H-2 proton of GlcNAc or glucosamine (GlcN) residues, respectively. The ring protons (H-3, -4, -5, and -6) of the control CS were considered to resonate at 3.1–3.9 ppm. The peaks at 4.6 and 4.8 ppm were assigned to the H-1 protons of the GlcN and GlcNAc residues, respectively.[34,35] The ^{1}H-NMR spectrum of 12-CS showed new peaks at 0.54, 0.95, 1.2, 1.9, 3.0, 3.1–3.9 (overlapping with the ring protons), and 4.5 ppm, which were assigned to the lauroyl protons [Fig. 3(b)]. The degree of substitution in *N*-acyl CSs ranged from 74.4% to 81.6%.[15]

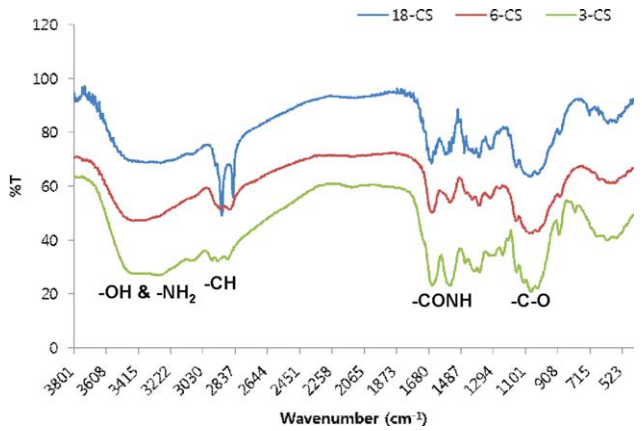

Figure 2 FTIR spectra of *N*-acyl CSs (3-CS, 6-CS, and 18-CS). [Color figure can be viewed in the online issue, which is available at wileyonlinelibrary.com.]

Critical aggregation concentration

To investigate the threshold concentration of self-aggregation formation, the critical aggregation concentration (CAC) was determined by observing the change in the intensity ratio of the pyrene in the presence of *N*-acyl CS. With increasing concentration of *N*-acyl CS, the total emission intensity increased, indicating that the probe transferred from the aqueous medium to the less polar micro-domains such as the interior of the self-aggregated NPs. Figure 4 exhibits the change of I_{372}/I_{389} value as a function of *N*-acyl CS concentration. The ratio of I_{372} to I_{389} was around 1.13 at the lower concentration and rarely changed until the concentration of *N*-acyl CS was 0.01 mg/mL. But, the ratio of I_{372} to I_{389} steadily decreased with further increase in the concentration of *N*-acyl CS due to the self-association of *N*-acyl CS. CAC was determined by the interception of two straight lines; its value was 0.01 mg/mL. This value did not change significantly between 3-CS and 18-CS because *N*-acyl hydrophobic alkyl chain elongations (MW up to 268) are much shorter than the polymeric chitosan backbone (MW 5.23×10^5).

Particle size distribution and surface morphology

Figure 5 shows the size distribution of the BSA-loaded lauroyl CNSP(12-CSNP). The particle size ranged from 55 to 310 nm and the average size was 138 nm. Table I shows the mean particle size of the 0.1 mg/mL BSA-loaded *N*-acyl CSNPs as a function of hydrophobic alkyl chain elongation. Generally, the mean particle size increased with hydrophobic alkyl chain elongation, suggesting that the elongation

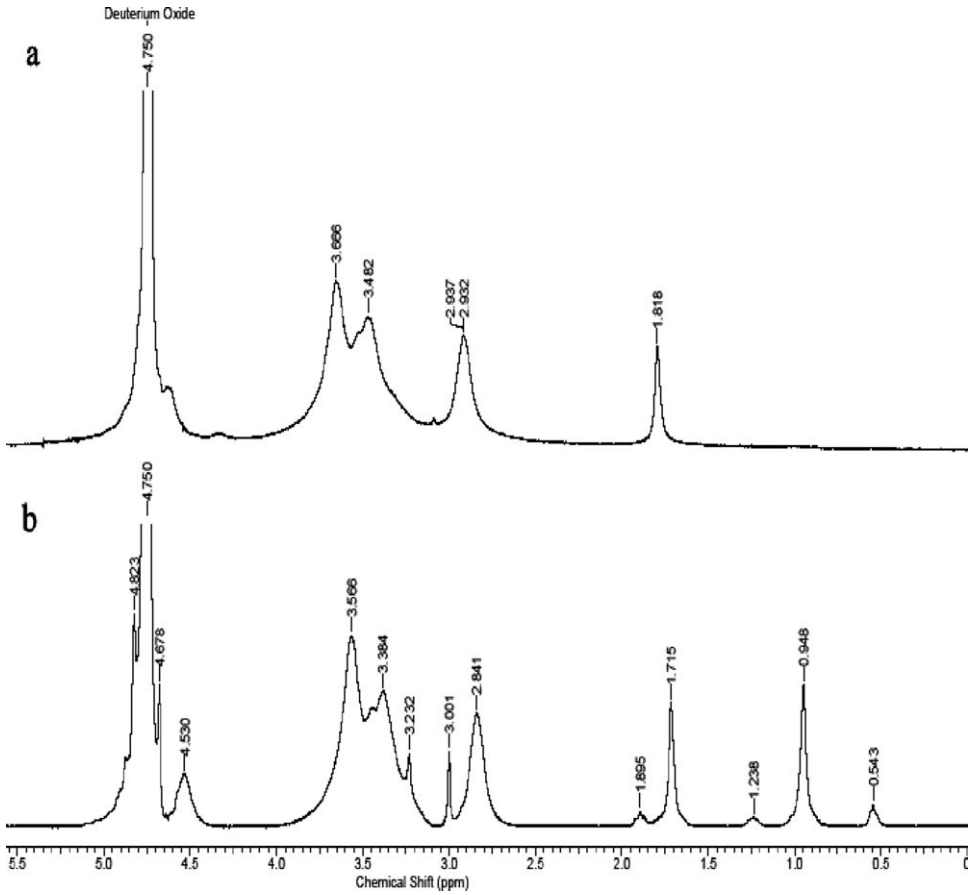

Figure 3 ^{1}H-NMR spectra of CS (a) and *N*-acyl CS (12-CS) (b) in CD_3COOD/deuterium oxide.

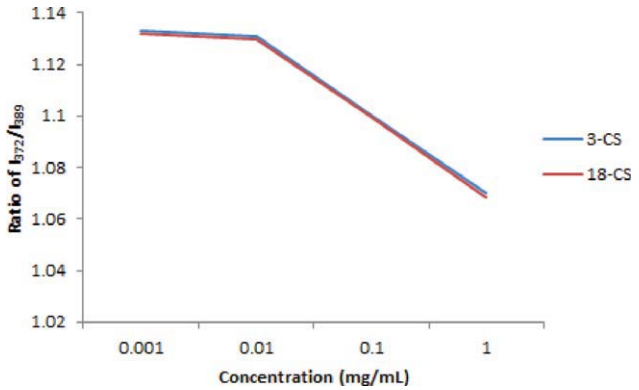

Figure 4 Plot of the I_{372}/I_{389} intensity ratio from the fluorescence spectra. [Color figure can be viewed in the online issue, which is available at wileyonlinelibrary.com.]

of hydrophobic side chain boosts the hydrophobic core in the CSNPs. Particle sizes of 12-CSNP and 15-CSNP were, however, sharply reduced to 138 nm and 159 nm, respectively. In both 12-CSNP and 15-CSNP, *N*-acyl CS might more tightly interact with BSA, resulting in decreased particle size. Table II shows the particle size of the BSA-loaded *N*-acyl CSNPs (3-CSNP and 12-CSNP) with BSA concentrations ranging from 0.1 to 1.0 mg/mL. With increasing BSA concentration, the particle sizes of the BSA loaded 3-CSNP and 12-CSNP increased due to the growth of the core. The surface morphology of the BSA-loaded *N*-acyl CSNPs was characterized by SEM. The BSA loaded 12-CSNPs displayed wrinkled surfaces and did not form complete spheres (Fig. 6). They were well-matched to the particle size distribution results.

Protein loading efficiency of *N*-acyl CSNPs

Table III summarizes the data on BSA loading efficiency of *N*-acyl CSNPs with BSA concentrations ranging from 0.1 to 1.0 mg/mL. Although BSA loading amounts in *N*-acyl CSNPs increased significantly with increasing BSA concentration, BSA loading efficiency decreased significantly with increasing BSA concentration. It is common that protein loading efficiency in nanoparticles decreased with increasing protein concentration because the amount of free

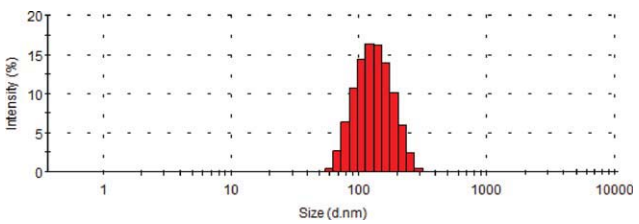

Figure 5 Size distribution of BSA-loaded lauroyl CSNPs (12-CS) in intensity. [Color figure can be viewed in the online issue, which is available at wileyonlinelibrary.com.]

TABLE I
The Mean Particle Size of the Protein Loaded *N*-Acyl Chitosan Nanoparticles at the Concentration of BSA (0.1 mg/mL)

Nanoparticles	3-CS	6-CS	9-CS	12-CS	15-CS	18-CS
Mean particle size (nm)	336	361	365	138	159	551

(not encapsulated) protein could be increased with higher protein concentration [eq. (1)]. On the other hand, BSA loading efficiency increased with lower protein concentration because most protein could be encapsulated and the amount of free protein should be reduced. At a BSA concentration of 0.1 mg/mL, the loading efficiency was ~ 94% and did not significantly change with hydrophobic alkyl chain elongation. However, the loading efficiency was more significant at higher BSA concentration and ranged from 63.2 to 81.9% with 1.0 mg/mL. In the previous studies,[15,17] BSA loading efficiencies of tripolyphosphate (TPP) ionic crosslinked CSNPs or linoleic acid-modified CSNPs were less than 30% with higher BSA concentration. Although they could improve the stability of CSNPs by crosslinking or linolenic acid modification, both crosslinking and the linoleic acid side chain will be rigid. If the side chains are not flexible, it will be structurally limited to encapsulate more core materials. *N*-acyl-modified CSNPs, which have more flexible saturated alkyl side chains, however, showed two to three times higher BSA loading efficiency at higher BSA concentration compared to the linoleic acid-modified CSNPs or TPP ionic crosslinked CSNPs. The highest BSA loading efficiency was observed in 12-CSNPs and 15-CSNPs. Generally, the particle size of the CSNPs increases with *N*-acyl chain length and BSA loading amounts. In this study, 12-CSNPs to 15-CSNPs, however, showed much smaller particle size and the highest BSA loading efficiency compared to the others. With these acyl chains, CSNPs would be structurally arranged in the core by more interactions with protein molecules such as hydrogen bond and hydrophobic interaction resulting in reducing the particle size.[36] This result can suggest that the optimum *N*-acyl chain length of CSNPs ranged 12- to 15- to

TABLE II
The Mean Particle Size (nm) of the Protein Loaded *N*-Acyl Chitosan Nanoparticles at the Various Concentrations of BSA

	The initial concentration of BSA (mg/mL)			
Nanoparticles	0.10	0.20	0.50	1.0
3-CS	336	376	479	484
12-CS	138	171	207	248

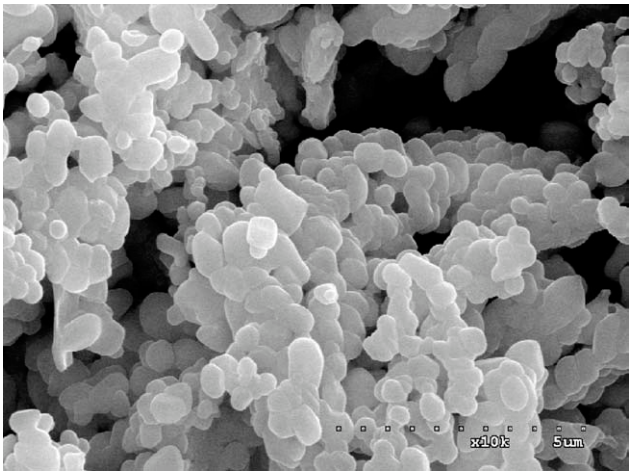

Figure 6 SEM of BSA loaded lauroyl CSNPs (12-CS). The micrograph is displayed at a magnification of ×10,000.

TABLE III
BSA Loading Efficiency of *N*-Acyl Chitosan Nanoparticles with Various Hydrophobic Carbon Chain Elongation

N-acyl chitosan nanoparticles	The concentration of BSA (mg/mL)			
	0.10	0.20	0.50	1.0
3-CS	94.3 ± 0.1	90.2 ± 0.2	80.8 ± 0.3	67.7 ± 0.2
6-CS	94.3 ± 0.1	90.3 ± 0.4	83.9 ± 0.9	78.8 ± 0.5
9-CS	94.7 ± 0.1	91.3 ± 0.6	81.3 ± 0.3	63.2 ± 0.4
12-CS	94.4 ± 0.2	90.4 ± 0.2	84.3 ± 0.2	81.6 ± 0.1
15-CS	94.3 ± 0.1	90.4 ± 0.1	85.6 ± 0.9	81.9 ± 0.6
18-CS	93.8 ± 0.2	89.3 ± 0.2	81.8 ± 0.2	74.2 ± 0.4

Values were means ($n = 3$) and the standard deviations, respectively.

obtain the highest BSA loading efficiency. The further study for the effect of acyl chain length on the structural arrangement inside the particle is underway.

CONCLUSIONS

N-acyl-modified CSNPs with various hydrophobic alkyl chain elongations from 3-CSNP to 18-CSNP were prepared by a self-aggregation method. *N*-acyl-modified CSNPs showed uniform spherical shape and their mean particle sizes ranged from 138 to 551 nm with hydrophobic alkyl chain elongation. BSA loading efficiency of CSNPs increased with *N*-acyl modification and the maximum loading efficiency at a higher BSA concentration (1.0 mg/mL) was observed with 12-CSNPs and 15-CSNPs. The results showed that *N*-acyl CSNPs have a great potential to increase the protein loading efficiency especially with higher protein concentration.

References

1. Wang, W. Int J Pharm 1999, 185, 129.
2. Chien, Y. W. Novel Drug Delivery Systems: Fundamentals, Developmental Concepts, Biomedical Assessments; Marcel Dekker: New York, 1982.
3. Lavasanifar, A.; Samuel, J.; Kwon, G. S. Adv Drug Delivery Rev 2002, 54, 169.
4. Liu, Z.; Jiao, Y.; Wang, Y.; Zhou, C.; Zhang, Z. Adv Drug Delivery Rev 2008, 60, 1650.
5. Tan, M. L.; Choong, P. F. M.; Dass, C. R. Peptides 2010, 31, 184.
6. Rao, S. V. R.; Shao, J. Int J Pharm 2008, 365, 2.
7. Dube, A.; Ng, K.; Nicolazzo, J. A.; Larson, I. Food Chem 2010, 122, 662.
8. Singh, R.; Lillard, J. W., Jr. Exp Mol Pathol 2009, 86, 215.
9. Kaul, G.; Amiji, M. J Pharm Sci 2005, 94, 184.
10. Xia, X.; Hu, Z.; Marquez, M. J Controlled Release 2005, 103, 21.
11. Dyer, A. M.; Hinchcliffe, M.; Watts, P.; Castile, J.; Jabbal-Gill, I.; Nankervis, R.; Smith, A.; Illum, L. Pharmacol Res 2002, 19, 998.
12. Cui, Z.; Mumper, R. J. J Controlled Release 2001, 75, 409.
13. Ma, Z.; Yeoh, H. H.; Lim, L. Y. J Pharm Sci 2002, 91, 1396.
14. Bozkir, A.; Saka, O. M. Drug Delivery 2004, 11, 107.
15. Liu, C. G.; Desai, K. G. H.; Chen, X. G.; Park, H. J. J Agric Food Chem 2005, 53, 437.
16. Liu, C. G.; Desai, K. G. H.; Chen, X. G.; Park, H. J. J Agric Food Chem 2005, 53, 1728.
17. Desai, K. G. H.; Park, H. J Drug Delivery 2006, 13, 375.
18. Roberts, G. A. F. Chitin Chemistry. The Mac Millan Press; London, 1992; p 274.
19. Soane, R. J.; Frier, M.; Perkins, A. C.; Jones, N. S.; Davis, S. S.; Illum, L. Int J Pharm 1999, 178, 55.
20. Illum, L. Pharmacol Res 1998, 15, 1326.
21. Dodane, V.; Vilivalam, D. Pharm Sci Technol Today 1998, 1, 246.
22. Paul, W.; Sharma, C. Pharm Sci 2000, 10, 5.
23. Dumitriu, S.; Chornet, E. Adv Drug Delivery Rev 1998, 31, 223.
24. Liu, X.; Chen, D.; Xie, L.; Zhang, R. J Controlled Release 2003, 93, 293.
25. Blanco, D.; Alonso, M. J. Eur J Pharm Biopharm 1997, 43, 287.
26. Tobío, M.; Gref, R.; Sanchez, A.; Langer, R.; Alonso, M. J Pharm Res 1998, 15, 270.
27. Tobío, M.; Sanchez, A.; Vila, A.; Soriano, I.; Evora, C.; Vila-Jato, J. L. Colloids Surf B 2000, 18, 315.
28. Ravi Kumar, M. N. V.; Bakowsky, U.; Lehr, C. M. Biomaterials 2004, 25, 1771.
29. Du, J.; Sun, R.; Zhang, S.; Govender, T.; Zhang, L. F.; Xiong, C. D.; Peng, Y. X. Macromol Rapid Commun 2004, 25, 954.
30. Lee, K. Y.; Ha, W. S.; Park, W. H. Biomaterials 1995, 16, 1211.
31. Moore, G. K.; Roberts, G. A. F. Int J Biol Macromol 1980, 2, 115.
32. Lavertu, M.; Xia, Z.; Serreqi, A. N.; Berrada, M.; Rodrigues, A.; Wang, D.; Buschmann, M. D.; Gupta, A. J Pharm Biomed Anal 2003, 32, 1149.
33. Shigemasa, Y.; Matsuura, H.; Sashiwa, H.; Saimoto, H. Int J Biol Macromol 1996, 18, 237.
34. Signini, R.; Campara Filho, S. P. Polym Bull 1999, 42, 159.
35. Sashiwa, H.; Kawasaki, N.; Nakayama, A.; Muraki, E.; Yamamoto, N.; Aiba, S. Biomacromolecules 2002, 3, 1126.
36. Zhu, A. P.; Yuan, L. H.; Chen, T.; Wu, H.; Zhao, F. Carbohydr Polym 2007, 69, 363.